ADVANCES IN ATMOSPHERIC SCIENCES, VOL. 31, SEPTEMBER 2014, 1113–1126

The Impacts of Two Types of El Niño on Global Ozone Variations in the Last Three Decades

XIE Fei[1], LI Jianping*[1], TIAN Wenshou[2], ZHANG Jiankai[2], and SHU Jianchuan[3]

[1]*State Key Laboratory of Numerical Modeling for Atmospheric Sciences and Geophysical Fluid Dynamics, Institute of Atmospheric Physics, Chinese Academy of Sciences, Beijing* 100029

[2]*Key Laboratory for Semi-Arid Climate Change of the Ministry of Education, College of Atmospheric Sciences, Lanzhou University, Lanzhou* 730000

[3]*Institute of Plateau Meteorology, China Meteorological Administration, Chengdu* 610072

(Received 19 August 2013; revised 27 December 2013; accepted 30 December 2013)

ABSTRACT

The effects of El Niño Modoki events on global ozone concentrations are investigated from 1980 to 2010 El Niño Modoki events cause a stronger Brewer–Dobson (BD) circulation which can transports more ozone-poor air from the troposphere to stratosphere, leading to a decrease of ozone in the lower-middle stratosphere from 90°S to 90°N. These changes in ozone concentrations reduce stratospheric column ozone. The reduction in stratospheric column ozone during El Niño Modoki events is more pronounced over the tropical eastern Pacific than over other tropical areas because transport of ozone-poor air from middle–high latitudes in both hemispheres to low latitudes is the strongest between 60°W and 120°W. Because of the decrease in stratospheric column ozone during El Niño Modoki events more UV radiation reaches the tropical troposphere leading to significant increases in tropospheric column ozone An empirical orthogonal function (EOF) analysis of the time series from 1980 to 2010 of stratospheric and tropospheric ozone monthly anomalies reveals that: El Niño Modoki events are associated with the primary EOF modes of both time series. We also found that El Niño Modoki events can affect global ozone more significantly than canonical El Niño events. These results imply that El Niño Modoki is a key contributor to variations in global ozone from 1980 to 2010.

Key words: stratospheric ozone, tropospheric ozone, canonical El Niño, El Niño Modoki

Citation: Xie, F., J. P. Li, W. S. Tian, J. K. Zhang, and J. C. Shu, 2014: The impacts of two types of El Niño on global ozone variations in the last three decades. *Adv. Atmos. Sci.*, **31**(5), 1113–1126, doi: 10.1007/s00376-013-3166-0.

1. Introduction

Stratospheric ozone concentrations directly affect levels of ultraviolet (UV) radiation reaching the Earth's surface and stratospheric temperature structure, while tropospheric ozone is considered to be a harmful air pollutant. Thus, the character, distribution and impact of ozone have been broadly studied (e.g., Chen et al., 1998, 2002, 2005, 2006; Hu and Tung, 2003; Zheng et al., 2003a, 2003b; Bian et al., 2005, 2006, 2007; Shi et al., 2007, 2010; Liu et al., 2009a, 2009b, 2011; Eyring et al., 2010). Meanwhile, the factors controlling ozone changes have always constituted an important research topic.

The canonical El Niño is the most significant mode of variation in the atmosphere. It can be derived from the first mode of an empirical orthogonal function (EOF) analysis of tropical Pacific Ocean SST (e.g., Rasmusson and Carpenter, 1982; Trenberth, 1997; Zhang et al., 2009). Canonical El Niño can cause anomalous propagation and dissipation of ultralong Rossby waves to impact the stratosphere at middle latitudes (van Loon and Labitzke, 1987; Hamilton, 1993; Sassi et al., 2004; García-Herrera et al., 2006; Manzini et al., 2006; Taguchi and Hartmann, 2006; Camp and Tung, 2007; Garfinkel and Hartmann, 2007; Free and Seidel, 2009; Xie et al., 2011) and influences the troposphere by adjusting the spatial distribution of convection (Reid and Gage, 1985; Philander, 1990; Yulaeva et al., 1994; Newell et al., 1996; Chandra et al., 1998; Randel et al., 2000; Gettelman et al., 2001; Kiladis et al., 2001; Sassi et al., 2004). Thus, canonical El Niño can influence the global ozone distribution by causing these circulation changes.

Based on an analysis of a global chemistry–climate model simulation of the atmosphere forced by observed SST variations and Stratospheric Aerosol and Gas Experiment II (SAGE II) observations of atmospheric composition, Randel et al. (2009) concluded that canonical El Niño events are tied to fluctuations in tropical upwelling. These fluctu-

* Corresponding author: LI Jianping
Email: ljp@lasg.iap.ac.cn

ations in tropical upwelling are linked to coherent anomalies in zonal mean temperature and ozone in the tropical lower stratosphere. Using a multiple regression method, Hood et al. (2010) found that canonical El Niño is associated with reduced ozone in the lower stratosphere and increased ozone in the middle stratosphere. The response of stratospheric ozone to canonical El Niño has also been analyzed using a variety of chemistry–climate models (Fischer et al., 2008; Cagnazzo et al., 2009) and a chemical transport model (Sassi et al., 2004). Recently, Randel and Thompson (2011) identified canonical El Niño as one of the main factors controlling variations in stratospheric ozone. In the troposphere, canonical El Niño events are associated with dryness, downward motion and suppressed convection in the tropical western Pacific over Indonesia. These changes are associated with an increase in tropospheric column ozone both because dryness increases the chemical lifetime of ozone and because the suppression of convection leads to weakened vertical transport of near-surface ozone. By contrast, in the eastern Pacific, increased humidity and enhanced upward transport result in a negative tropospheric column ozone anomaly (e.g., Kley et al., 1996; Chandra et al., 1998; Hauglustaine et al., 1999; Thompson and Hudson, 1999; Fujiwara et al., 2000; Sudo and Takahashi, 2001; Thompson et al., 2001; Chandra et al., 2002, 2007, 2009; Ziemke and Chandra, 2003, Ziemke et al., 2010; Doherty et al., 2006; Oman et al., 2011). Moreover, several previous studies have pointed out that changes of stratosphere–troposphere exchange (STE) caused by canonical El Niño also significantly affect ozone concentrations in the extratropical troposphere (Langford et al., 1998; James et al., 2003; Zeng and Pyle, 2005).

The second leading mode of an EOF analysis of tropical Pacific Ocean SST variability from 1980 to 2010 shows two cold centers in the eastern and western Pacific and a warm center in the central Pacific (Fig. 1b), referred to as El Niño Modoki, compared with a cold center in the eastern Pacific and a warm center in the western Pacific in canonical El Niño events (Fig. 1a) (Ashok et al., 2007). Since the late 1970s, the number of El Nino Modoki events has been increasing (Ashok and Yamagata, 2009; Yeh et al., 2009). However, the impacts of El Niño Modoki on ozone changes do not receive a lot of attention.

Canonical El Niño and El Niño Modoki events can lead to profoundly different effects on stratospheric temperature and circulation (Hu and Fu, 2009; Hu and Pan, 2009; Hurwitz et al., 2011a, 2011b; Lin et al., 2012; Xie et al., 2012; Zubiaurre and Calvo, 2012). This is because, in the mid-latitude stratosphere, the gradient patterns of sea surface temperature anomalies (SSTAs) in the two types of El Niño events can cause completely different patterns of propagation and dissipation of ultralong Rossby waves. Trenberth and Smith (2006, 2009) noted that the two types of El Niño result in distinct temperature anomalies in the high-latitude stratosphere in the Southern Hemisphere. Xie et al. (2012) pointed out that zonal circulation changes are completely different in the two types of El Niño in the middle–high-latitude stratosphere, i.e., canonical El Niño events weaken and warm the north polar vortex but strengthen and cool the south polar vortex; however, El Niño Modoki events strengthen and cool the north polar vortex but weaken and warm the south polar vortex. Ashok et al. (2007) found that a tripolar pattern of sea level pressure anomalies appears in the evolution of El Niño Modoki events where the centers of the tripolar pattern locate in the tropical western Pacific, central Pacific and eastern Pacific; and in El Niño Modoki events there are two anomalous Walker circulation cells (compared with the single cell related to canonical El Niño events).

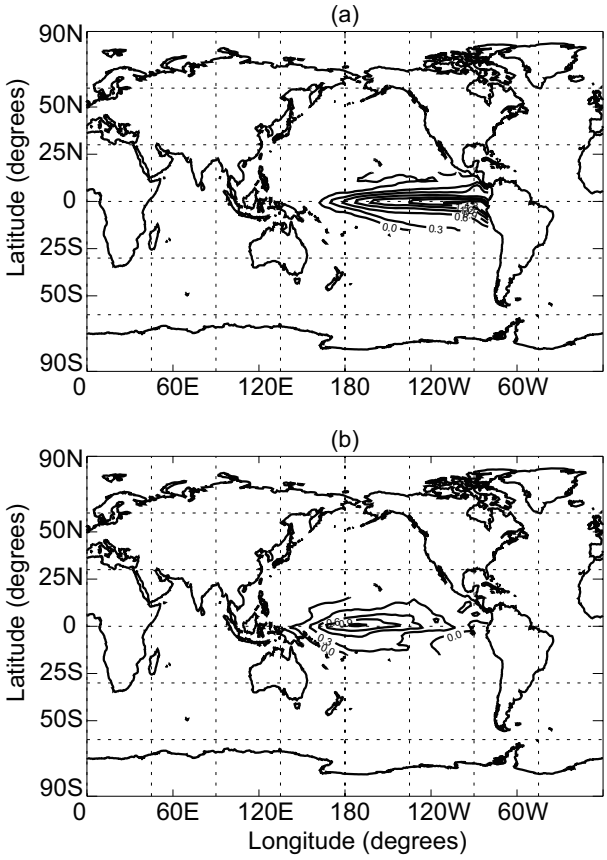

Fig. 1. SSTAs in the tropical Pacific Ocean during (a) canonical El Niño events and (b) El Niño Modoki events. Solid lines represent positive values. Contour lines are $\pm 0.3^{\circ}$C.

During El Niño Modoki events, the anomalies in the atmospheric circulation seem to affect the stratosphere and troposphere differently from those associated with canonical El Niño events. Thus, global stratospheric and tropospheric ozone may respond differently to the two types of El Niño events. This study not only investigates the different effects of the two types of El Niño on global ozone, but also tries to explain the mechanisms underlying these effects. The manuscript is organized as follows. Section 2 describes the data and numerical simulations used in the study. Section 3 discusses the relationships between patterns of stratospheric ozone changes and the two types of El Niño, and section 4 analyzes the variations in tropospheric ozone patterns associated with the two types of El Niño. Conclusions are presented in section 5.

2. Data and methods

Ozone is taken from monthly mean European Center for Medium Range Weather Forecasting (ECMWF) reanalysis data (ERA-Interim) between 1980 and 2010 (Simmons et al., 2007a, b; Uppala et al., 2008). ERA-Interim has assimilated satellite observations (reprocessed Global Ozone Monitoring Experiment data from the Rutherford Appleton Laboratory provides ozone profile information from 1995 onwards) at a $1.5^\circ \times 1.5^\circ$ horizontal resolution and relatively high vertical resolution (37 levels) compared with the ERA40 reanalysis (23 levels) (Simmons et al., 2007a, b; Uppala et al., 2008). Figure 2 shows the longitude–latitude cross sections of zonally-averaged ozone (averaged over 2005–2010) from ERA-Interim and the Aura Microwave Limb Sounder (MLS), horizontal distributions of ERA-Interim total column ozone (TCO) (averaged over 1980–2010) and assimilated observed TCO from the National Institute of Water and Atmospheric Research (NIWA) (averaged over 1980–2009) (Bodeker et al., 2005), and the time series of ERA-Interim and NIWA TCO averaged for the latitude band of 50°S–50°N. The averaged latitude range of this limitation is dictated by the number of missing values in the NIWA TCO at high latitudes, so that ERA-Interim and NIWA TCO can only be compared at lower–middle latitudes. The spatial distribution and time series of ERA-Interim ozone agree well with ozone observed

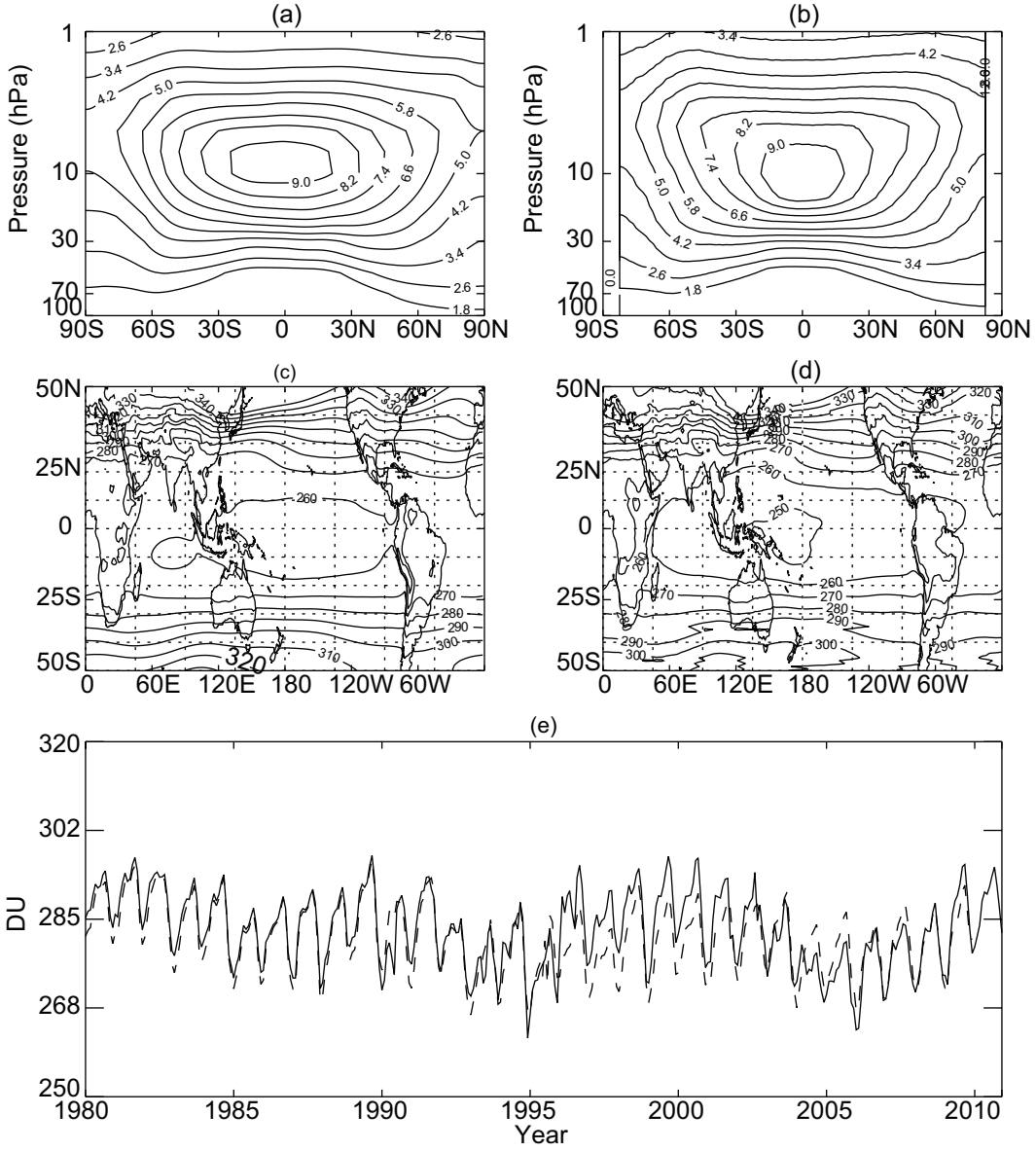

Fig. 2. Longitude–latitude cross sections of zonally-averaged ozone (averaged over 2005–2010) from (a) ERA-Interim ozone and (b) Aura MLS ozone. Contour intervals are 1.8 ppmv. Total column ozone (TCO) distributions (c) based on ERA-Interim data averaged over the period 1980–2010 and (d) based on NIWA data averaged over the period 1980–2009. Contour intervals are 10 DU. (e) Time series of ERA-interim (solid line) and NIWA (dashed line) TCO averaged over (50°S–50°N, 180°W–180°E).

by the Aura MLS and NIWA. Dragani (2011) also compared ERA-Interim ozone with satellite data and concluded that the ERA-Interim data are reasonable and realistic. ERA-Interim ozone data are therefore suitable for diagnosing spatial and temporal ozone anomalies.

To identify occurrences of El Niño Modoki and canonical El Niño events, we use the monthly ENSO Modoki index, hereafter EMI, and the NINO3 index, hereafter N3I, respectively. The EMI is defined as follows, according to Ashok et al. (2007):

$$\mathrm{EMI} = (\mathrm{SSTA})_{\mathrm{C}} - 0.5 \times (\mathrm{SSTA})_{\mathrm{E}} - 0.5 \times (\mathrm{SSTA})_{\mathrm{W}} ,$$

where the subscripted brackets is the area mean SSTA over the central Pacific area [$(\mathrm{SSTA})_{\mathrm{C}}$: (10°S–10°N, 165°E–140°W)], the eastern Pacific area [$(\mathrm{SSTA})_{\mathrm{E}}$: (15°S–5°N, 110°–70°W)], and the western Pacific area [$(\mathrm{SSTA})_{\mathrm{W}}$: (10°S–20°N, 125°–145°E)]. N3I is defined as the area-mean SSTA over the region (5°S–5°N, 150°–90°W), and is available at http://www.cpc.noaa.gov/data/indices/. Following previous studies (Weng et al., 2009; Zhang et al., 2010; Feng and Li, 2011), months with EMI values equal to or greater than +0.5°C were identified as El Niño Modoki events. Similarly, months with N3I values equal to or greater than +0.5°C were identified as El Niño events. Several strong and continuous El Niño samples have been selected for this study (Table 1).

The formulae to calculate the Brewer–Dobson (BD) circulation in a pressure coordinate system were given by Edmon et al. (1980):

$$\bar{v}^{*} = \bar{v} - [\overline{(v'\theta')}/\bar{\theta}_p]_p ,$$
$$\bar{\omega}^{*} = \bar{\omega} + (a\cos\phi)^{-1}[\cos\phi(\overline{(v'\theta')}/\bar{\theta}_p)]_\phi ,$$

where θ is the potential temperature; a is the radius of the earth; $\bar{v}$ is mean meridional wind; and $\bar{\omega}$ is mean vertical velocity in pressure coordinates. Subscripts p and ϕ denote derivatives with pressure p and latitude ϕ, respectively. The overbar denotes the zonal mean and the accent denotes the deviations from the zonal mean value.

3. The different impacts on stratospheric ozone

Figure 3 shows latitude–height cross sections of ozone anomalies above 100 hPa associated with canonical El Niño and El Niño Modoki events. Previous studies have shown that

Table 1. Samples of canonical El Niño (left column) and El Niño Modoki (right column) events from 1980 to 2010 analyzed in this paper.

Canonical El Niño	El Niño Modoki
Jul 1982–Aug 1983	Sep 1990–Dec 1991
Dec 1986–Jan 1988	Apr 1994–Jun 1995
May 1997–May 1998	Jun 2002–Apr 2003
Aug 2006–Jan 2007	Jun 2004–Dec 2004
	Oct 2009–Feb 2010

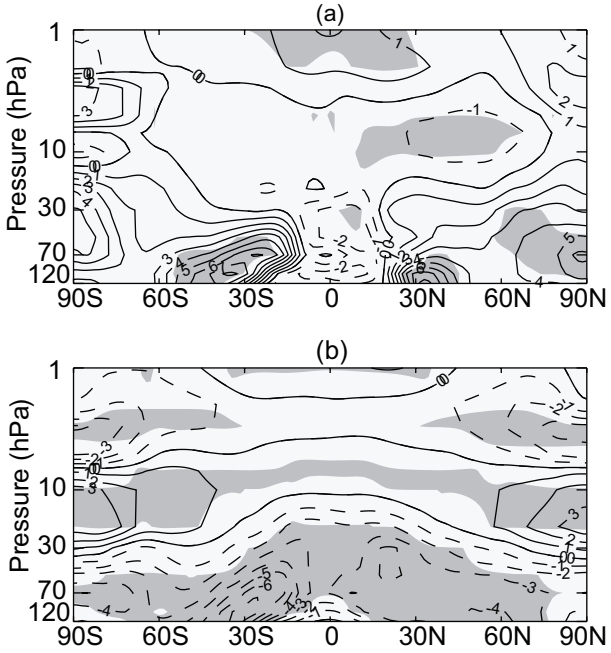

Fig. 3. Latitude–height cross sections of zonally-averaged stratospheric ozone anomalies (%) composited for (a) canonical El Niño events and (b) El Niño Modoki events based on ERA-Interim data from 1980 to 2010. Contour intervals are ±1% for ozone anomalies. Solid lines represent positive values; dashed lines represent negative values. Shaded areas are significant at the 95% confidence level (Student's *t*-test). The canonical El Niño anomalies are calculated using composites of the detrended and deseasonalized time series over the selected canonical El Niño events, just as the El Niño Modoki anomalies are calculated using composites over the selected El Niño Modoki events. For the selected canonical El Niño/El Niño Modoki events, please refer to Table 1. Before the composite analysis, the QBO signals in ozone were filtered out from time series using a 24–40-month band-pass filter.

warm ENSO events weaken the northern polar vortex, which increases ozone concentrations at high latitudes in the Northern Hemisphere (e.g., Fischer et al., 2008; Cagnazzo et al., 2009), and strengthen BD-related dynamical transport from the upper troposphere to the lower stratosphere in the tropics (e.g., Sassi et al., 2004; García-Herrera et al., 2006; Manzini et al., 2006; Calvo et al., 2010), which reduces ozone concentrations in the tropical lower stratosphere (Randel et al., 2009; Hood et al., 2010). In agreement with these previous studies, canonical El Niño events lead to a positive ozone anomaly at high latitudes in the Northern Hemisphere and a negative ozone anomaly in the tropical lower stratosphere and a positive ozone anomaly at high latitudes in the Southern Hemisphere (Fig. 3a). The pattern of circulation anomalies associated with El Niño Modoki is totally different from those associated with canonical El Niño (Xie et al., 2012), and hence the pattern of ozone anomalies associated with El Niño Modoki is also totally different from those associated with canonical El Niño i.e. El Niño Modoki activities reduce ozone in the lower-middle stratosphere over almost the entire globe and in

the upper stratosphere at high latitudes but increase ozone in the middle stratosphere at high latitudes (Fig. 3b). The ozone anomalies are arranged in a banded distribution.

Randel and Wu (1996) used a singular value decomposition (SVD) and regression analysis of observed stratospheric ozone from 1979 to 1995 to show that the first and second modes of the SVD are associated with the quasi-biennial oscillation (QBO) Together, these two dominant modes accounted for approximately 97% of the variance. More recently, Randel and Thompson (2011) reported that both QBO and ENSO have been major contributors to variations in stratospheric ozone. An EOF analysis of the stratospheric ozone 1980–2010 time series is used to isolate the QBO and ENSO signals in ozone over the past 30 years. The spatial and temporal variations of the first and second modes of this EOF analysis are shown in Fig. 4. The leading EOF spatial mode (EOF1; Fig. 4a), which accounts for 27% of the variance, corresponds to the El Niño Modoki pattern of strato-

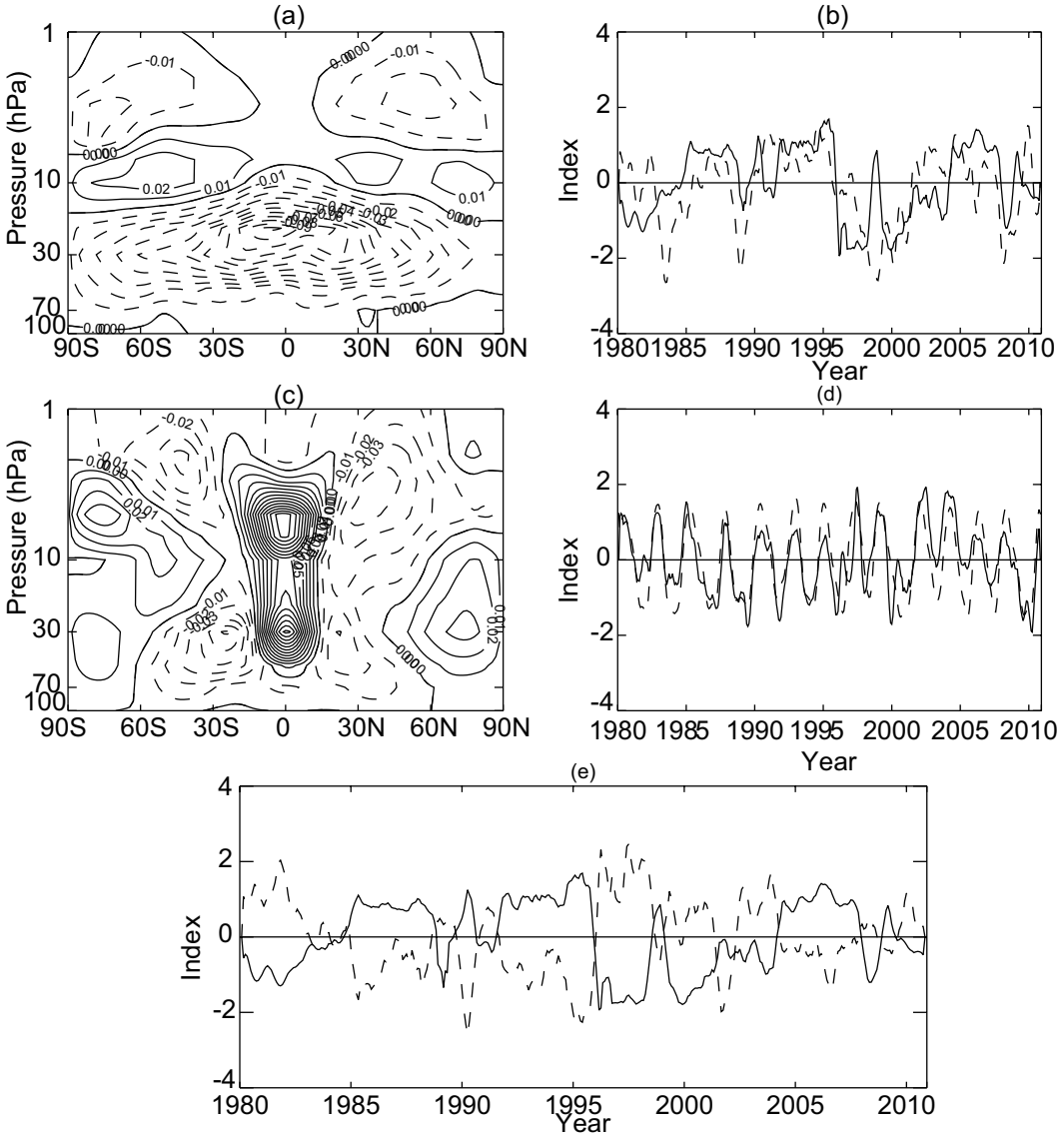

Fig. 4. Results of empirical orthogonal function (EOF) analysis of the 1980–2010 time series of zonally-averaged stratospheric ozone anomalies. The range for performing EOF analysis is from 100 hPa to 1 hPa and from 90°S to 90°N. The ozone anomalies were obtained by removing the annual cycle and linear trend from the original time series at each grid. The square-root of the cosine of latitude and square-root of the pressure interval was used for the weighting function in the EOF analysis. (a) The spatial pattern of the leading EOF mode (EOF1). Contour intervals are ± 0.01 ppmv. Solid lines represent positive values; dashed lines represent negative values. (b) The variations of the leading principal component (PC1; solid line) and EMI (dashed line). (c) As in (a), but for the spatial pattern of EOF2. (d) As in (b), but for the variations of PC2 (solid line) and the QBO index (dashed line). (e) The variations of PC1 (solid line) and mean stratospheric ozone anomalies (dashed line). All the time series are normalized.

spheric ozone anomalies (Fig. 3b). The variations of the leading principal component (PC1) are strongly correlated with EMI, with a linear correlation coefficient of 0.59 (Fig. 4b). The second spatial mode (EOF2; Fig. 4c) which accounts for 1% of the variance, is associated with the QBO pattern of ozone anomalies reported by previous studies (Randel and Wu, 1996; Lee and Smith, 2003; Crooks and Gray, 2005; Randel and Wu, 2007). Randel and Wu (1996) showed that the QBO signal in stratospheric ozone results from secondary circulations induced by the QBO. The variations of the second principal component (PC2) is significantly correlated with the QBO index (Fig. 4d), where the QBO index is defined as the normalized zonal wind at 30 hPa averaged between 10°S and 10°N. The linear correlation coefficient between PC2 and QBO index is 0.70 Figure 4 suggests that the impacts of El Niño Modoki on stratospheric ozone have exceeded those of the QBO over the past 30 years. The variations of mean ozone anomalies from 100 hPa to 1 hPa and the variations of PC1 are shown in Fig. 4e. The stratospheric ozone changes and PC1 are anti-correlated with a statistically significant linear correlation coefficient of -0.76 which is associated with El Niño Modoki activity. This strong anti-correlation implies that El Niño Modoki has played a key role in controlling variations of stratospheric ozone over the past three decades.

Previous studies have shown that El Niño activities tend to strengthen the Brewer–Dobson (BD) circulation in the tropical lower stratosphere, which transports the tropospheric low-ozone air to the stratosphere and causes a local ozone decrease in the tropical lower stratosphere (Randel et al., 2009; Hood et al., 2010). The lead-lag correlations (LLCs) between the vertical component of BD circulation, diagnosed from National Centers for Environmental Prediction Reanalysis 2 (NCEP2) and ERA-interim data, and EMI and N3I index shown in Figs. 5a and b illustrate that the BD circulation variations are more closely linked with El Niño Modoki events than with canonical El Niño events during the past three decades. This may be the reason that El Niño Modoki can cause more significant ozone decreases in the middle-lower stratosphere compared with canonical El Niño. Randel et al. (2009) and Hood et al. (2010) noted that El Niño tends to reduce ozone in the tropical lower stratosphere and increase ozone in the tropical middle stratosphere. These studies did not differentiate between the two types of El Niño; however, it is evident that ozone anomalies in the tropical stratosphere are larger during El Niño Modoki periods than during canonical El Niño periods. These results suggest that El Niño Modoki events have a more significant impact on ozone distributions in the lower and middle stratosphere than canonical El Niño. The decreased lower stratospheric ozone and the increased middle stratospheric ozone observed during El Niño events may be mainly related to El Niño Modoki, but not canonical El Niño.

Figure 3 indicates that the effects of both types of El Niño on stratospheric ozone vary significantly in the spatial domain. Stratospheric column ozone anomalies are calculated to better estimate the net effects of El Niño events on

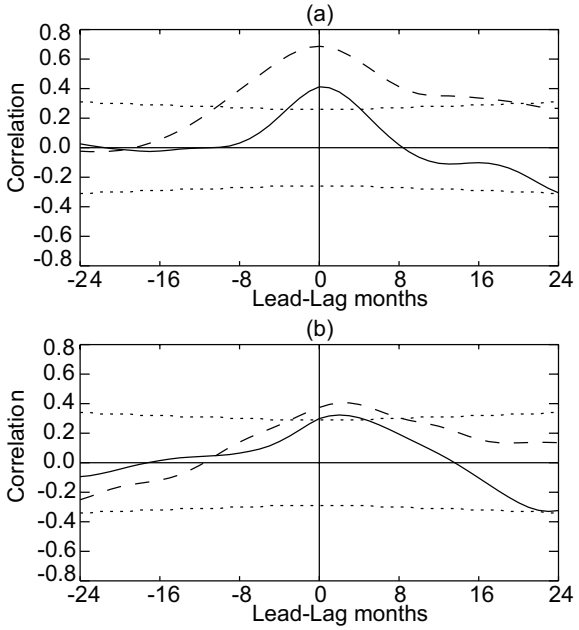

Fig. 5. (a) Lead-lag correlations (LLCs) between the vertical component of BD circulation and N3I (solid line) and EMI (dashed line) for the calculation of BD circulation from NCEP2 data. Mean area of BD circulation: (30°S–30°N, 180°W–180°E); 120 hPa–70 hPa. A positive lag means the EMI and N3I lead, and a negative lag means BD circulation leads. The dotted lines denote the 95% confidence level. (b) Same as (a), but the calculation of BD circulation is from ERA-interim data.

total stratospheric ozone. These stratospheric column ozone anomalies are shown in Fig. 6. Stratospheric column ozone is calculated assuming that the stratosphere extends from the tropopause to 1 hPa. The tropopause is determined using the World Meteorological Organization (WMO) definition (thermal tropopause) in the tropics, the 2.5 PV pressure level (dynamic tropopause) at high latitudes, and a weighted average of the thermal and dynamic tropopauses (mixed tropopause) in middle latitudes. Canonical El Niño causes significant increases in stratospheric column ozone at middle–high latitudes in the Northern Hemisphere (Fig. 6a) because it weakens the Northern Hemisphere polar vortex. By contrast, canonical El Niño causes decreases in stratospheric column ozone in the tropics because it strengthens the BD circulation. Stratospheric column ozone also increases over the Southern Hemisphere middle–high latitudes, with the exception of a negative stratospheric column ozone anomaly between 60°E and 180°E. Stratospheric column ozone anomalies associated with El Niño Modoki are completely different from those associated with canonical El Niño. El Niño Modoki reduces global stratospheric column ozone (Fig. 6b). This is because El Niño Modoki events significantly decrease the lower-middle stratospheric ozone (Fig. 3b). The results also agree with the above if stratospheric column ozone is calculated assuming that the stratosphere extends from 200 to 1 hPa.

It is noteworthy that El Niño Modoki causes a more significant decrease in stratospheric column ozone over the trop-

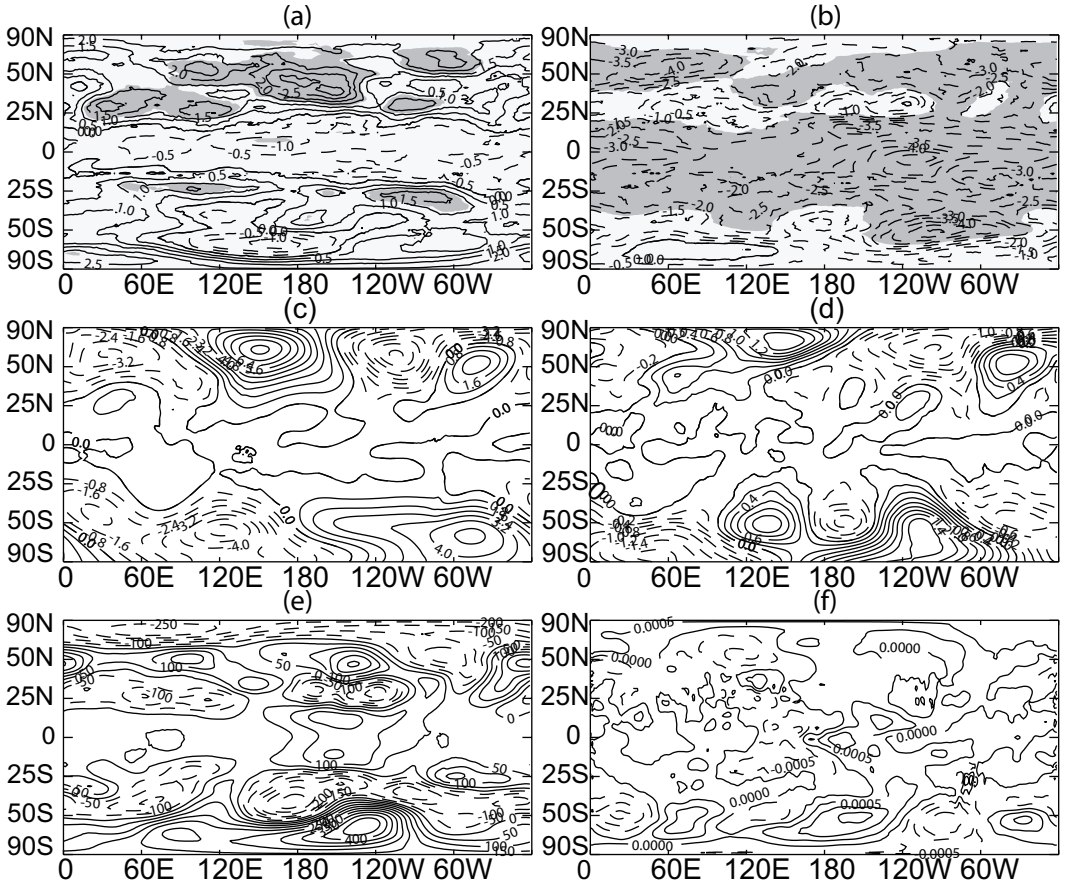

Fig. 6. Latitude–longitude cross sections of stratospheric column ozone anomalies (%) composited from 1980–2010 ERA-Interim data for (a) canonical El Niño events and (b) El Niño Modoki events. Contour intervals are ±0.5% for ozone anomalies. Solid lines represent positive values; dashed lines represent negative values. Stratospheric column ozone is calculated assuming that the stratosphere extends from the tropopause to 1 hPa. Shaded areas are significant at the 95% confidence level (Student's *t*-test). Latitude–longitude cross sections of climatological lower-stratospheric meridional winds averaged from 100 hPa to 30 hPa based on (c) ERA-Interim data from 1980 to 2010. Contour intervals are 0.8 m s^{-1}. Solid lines represent northerly vectors; dashed lines represent southerly vectors. (d) Latitude–longitude cross section of anomalies of lower-stratospheric meridional wind composited for El Niño Modoki events based on ERA-Interim data from 1980 to 2010. Contour intervals are 0.2 m s^{-1}. Solid lines represent positive values; dashed lines represent negative values. (e) Same as (d), but for upper-tropospheric-averaged (300–100 hPa) geopotential. Contour intervals are 50 m^2 s^{-2}. (f) Same as (d), but for lower-stratospheric-averaged (100–50 hPa) vertical velocity. Contour intervals are 0.00005 Pa s^{-1}.

ical eastern Pacific (60°–120°W) than over other tropical areas (Fig. 6b). This decrease is particularly pronounced in the Southern Hemisphere tropical eastern Pacific. Further analysis of reanalysis data indicates that the decrease of lower-stratospheric ozone (averaged between 100 hPa and 30 hPa) during El Niño Modoki periods is most significant over the tropical eastern Pacific, particularly the Southern Hemisphere tropical eastern Pacific (not shown). The spatial pattern of anomalies in lower-stratospheric ozone concentrations is similar to that of anomalies in stratospheric column ozone.

Dynamical transport plays an important role in controlling the spatial distribution of ozone in the stratosphere. Figure 6c shows climatologies of lower-stratospheric meridional wind and El Niño Modoki anomalies of lower-stratospheric meridional wind (Fig. 6d) averaged between 100 hPa and 30 hPa from reanalysis data. It illustrates that the meridional wind is directed from middle–high latitudes to lower latitudes in both hemispheres throughout the longitude band of 60°–120°W (Fig. 6c). We found the equatorward wind in this longitude band is further enhanced during El Niño Modoki events, particularly in the Southern Hemisphere (Fig. 6d). Renwick and Revell (1999) pointed out that these significant meridional wind anomalies in middle–high latitudes are likely to be related to blocking over the south Pacific and Rossby wave propagation during ENSO events. It is indeed found that there is a positive anomaly of geopotential, which represents an abnormal high pressure center, near the longitude of 120°W in the Southern Hemisphere high latitudes (Fig. 6e). The anomalous equatorward meridional wind during El Niño Modoki periods brings more ozone-poor air from

the middle–high-latitude lower stratosphere to the tropical lower stratosphere in the longitude band of 60°–120°W. Figure 6f shows that the vertical velocity over the tropical eastern Pacific (60°–120°W) is stronger in El Niño Modoki events. The intensity of vertical velocity would bring more ozone-poor air from the upper troposphere to the stratosphere. The anomalous horizontal and vertical transports reduce ozone concentrations in the tropical lower stratosphere over the longitude band of 60°–120°W, causing a significant reduction in stratospheric column ozone over the tropical eastern Pacific (60°–120°W) during El Niño Modoki periods (Fig. 6b). The strongest meridional wind anomalies over this longitude range occur in the Southern Hemisphere, so that the lowest ozone concentrations in the tropical region are located over the tropical eastern Pacific in the Southern Hemisphere.

4. The different impacts on tropospheric ozone

The radiation effect of tropospheric ozone has important impacts on climate (Liao et al., 2004, 2006; Liao and Seinfeld, 2005). ENSO activities dominate the variations of the Hadley cell (Quan et al., 2004), and have been shown to profoundly impact the Walker circulation by displacing areas of convective activity. These circulation changes influence the distribution of chemical constituents in the troposphere, including ozone (Chandra et al., 1998, 2009; Sudo and Takahashi, 2001; Chandra et al., 2002; Ziemke and Chandra, 2003; Zeng and Pyle, 2005; Doherty et al., 2006; Chandra et al., 2009; Lee et al., 2010; Randel and Thompson, 2011). Observations of TCO (Ziemke et al., 2010) and numerical simulations (Oman et al., 2011) indicate that the variations of ozone in the troposphere are dominated by the response to ENSO over the western and eastern Pacific. The impact of ENSO on tropospheric ozone has been extensively studied; however, changes in tropospheric ozone associated with El Niño Modoki have not yet been examined in detail.

Figure 7 shows latitude–height cross sections of composite ozone anomalies below 200 hPa associated with canonical El Niño (Fig. 7a) and El Niño Modoki (Fig. 7b). Canonical El Niño is associated with increased tropospheric ozone in the Southern Hemisphere. In the Northern Hemisphere, ozone is reduced in the lower troposphere but increased in the middle–upper troposphere (Fig. 7a). However, these effects of canonical El Niño events on tropospheric ozone are almost insignificant. El Niño Modoki is associated with a significant increase in ozone throughout the troposphere except for the north polar region, with a maximum increase in the middle troposphere at low latitudes.

The EOF analysis of the 1980–2010 time series of stratospheric ozone presented in section 3 indicates that El Niño Modoki plays a key role in determining stratospheric ozone variability. A similar EOF analysis is performed on the time series of tropospheric ozone over the same period Figure 8 shows the spatial and temporal variations of the first and

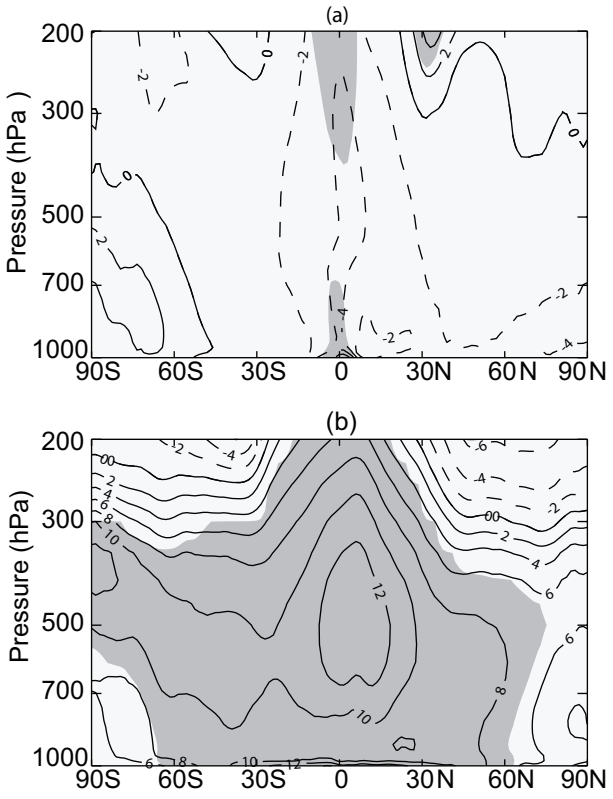

Fig. 7. The same as Fig. 3, but for zonally-averaged tropospheric ozone anomalies composited for (a) canonical El Niño events and (b) El Niño Modoki events.

second EOF modes of tropospheric ozone. The spatial pattern of EOF1 which accounts for 50% of the total variance, corresponds to tropospheric ozone anomalies during El Niño Modoki events (Figs. 8a and 7b). The variation of PC1 is likewise strongly correlated with EMI (Fig. 8b), with a linear correlation coefficient of 0.57 EOF2 is also significant accounting for 22% of the variance (Fig. 8c). It is found that the variation of PC2 is significantly anti-correlated with the variation of lower stratospheric ozone (Fig. 8d), with a linear correlation coefficient of -0.54 This anticorrelation implies that the second EOF mode may be associated with NO_x-related chemistry in the atmosphere, which has opposite effects on tropospheric and stratospheric ozone (NO_x creates tropospheric ozone but depletes stratospheric ozone). This may be why we found that variations of PC2 are significantly anticorrelated with the variations of lower-stratospheric ozone Figure 8 also indicates that El Niño Modoki has been the most important factor in determining tropospheric ozone variability over the past 30 years. Figure 8e shows the variations of PC1 and averaged tropospheric ozone anomalies Changes in tropospheric ozone are significantly correlated with PC1, which is associated with El Niño Modoki This correlation implies that El Niño Modoki also plays a key role in controlling the variations of tropospheric ozone over the past three decades.

Previous studies have demonstrated that ENSO changes the longitudinal distribution of tropospheric ozone at lower

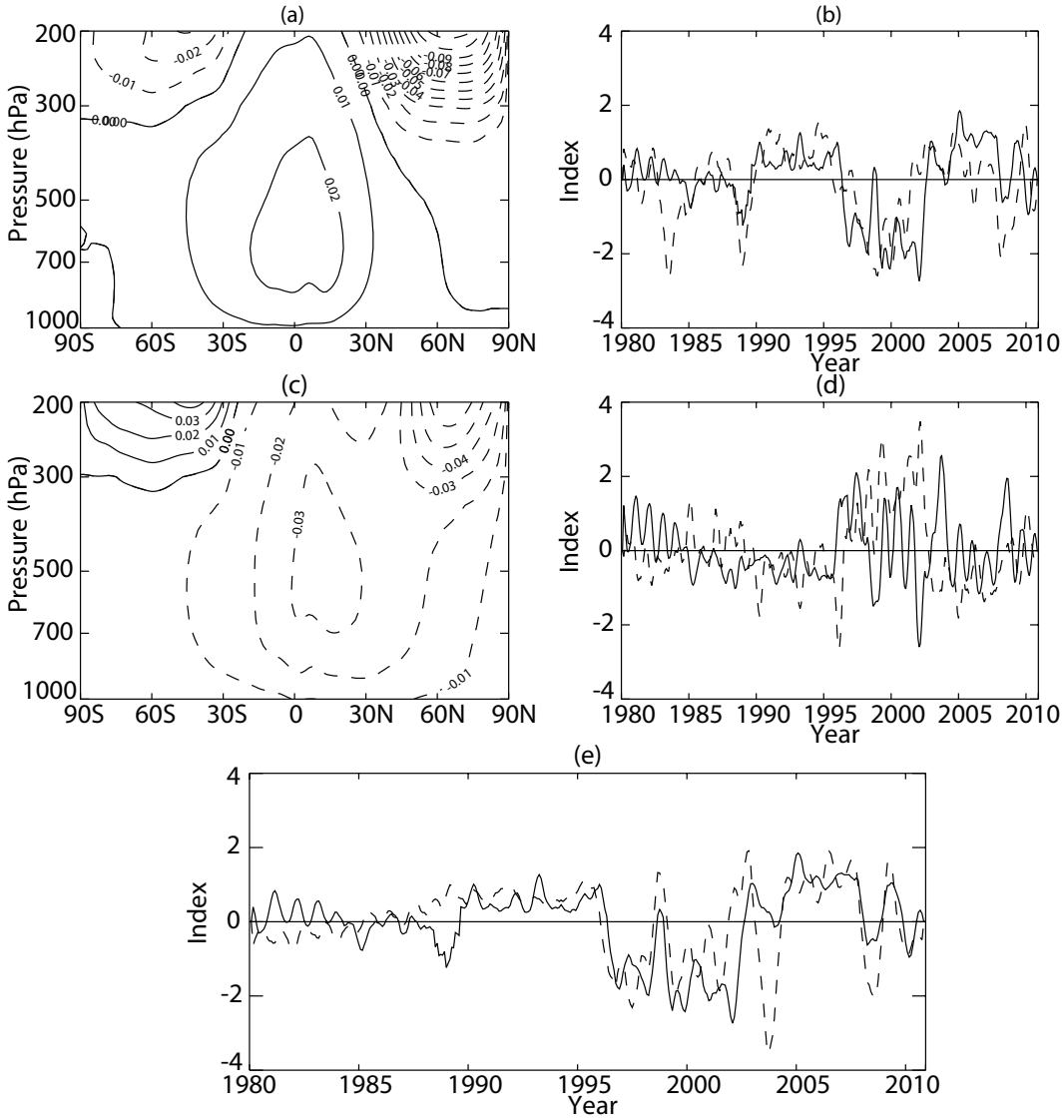

Fig. 8. The same as Fig. 4, but for zonally-averaged tropospheric ozone anomalies. The range for performing the EOF analysis is from 1000 hPa to 200 hPa and from 90°S to 90°N.

latitudes (Ziemke et al., 2010; Oman et al., 2011). Figure 9 shows anomalies in tropospheric column ozone associated with both types of El Niño events. Tropospheric column ozone is calculated assuming that the troposphere extends from the tropopause to 1000 hPa, where the tropopause is defined as in section 3. These cross sections allow further comparison and analysis of tropospheric ozone anomalies associated with the two types of El Niño events. Due to the effect of canonical El Niño on convection and Walker circulation, the tropospheric ozone anomalies associated with canonical El Niño are positive in the western Pacific but negative anomalies occur in the middle and eastern Pacific (Fig. 9a). These results are consistent with previous studies (e.g., Chandra et al., 1998; Thompson and Hudson, 1999; Ziemke et al., 2010; Oman et al., 2011). By contrast, El Niño Modoki is associated with a significant increase in ozone throughout the tropical troposphere, with a maximum increase over the central-eastern Pacific (Fig. 9b). Figure 9 indicates that the tropospheric ozone anomalies associated with El Niño Modoki are completely different from those associated with canonical El Niño. Figure 9 also illustrates that El Niño Modoki induces a more profound increase in tropical tropospheric ozone than canonical El Niño. The increases in tropospheric ozone at low latitudes are transported poleward, which may lead to ozone increases at whole middle latitudes in the Southern Hemisphere and over the longitude ranges of 0°–90°E and 0°–180°W of middle latitudes in the Northern Hemisphere during El Niño Modoki events. The next step is to understand how El Niño Modoki causes significant increases in ozone in the tropical troposphere. The results also agree with the above if tropospheric column ozone is calculated assuming that the troposphere extends from 200 hPa to 1000 hPa.

Tropospheric ozone concentrations are affected by stratosphere–troposphere exchange (STE), tropical convective activity, the amount of UV radiation reaching the troposphere, tropospheric water vapor concentration, and tro-

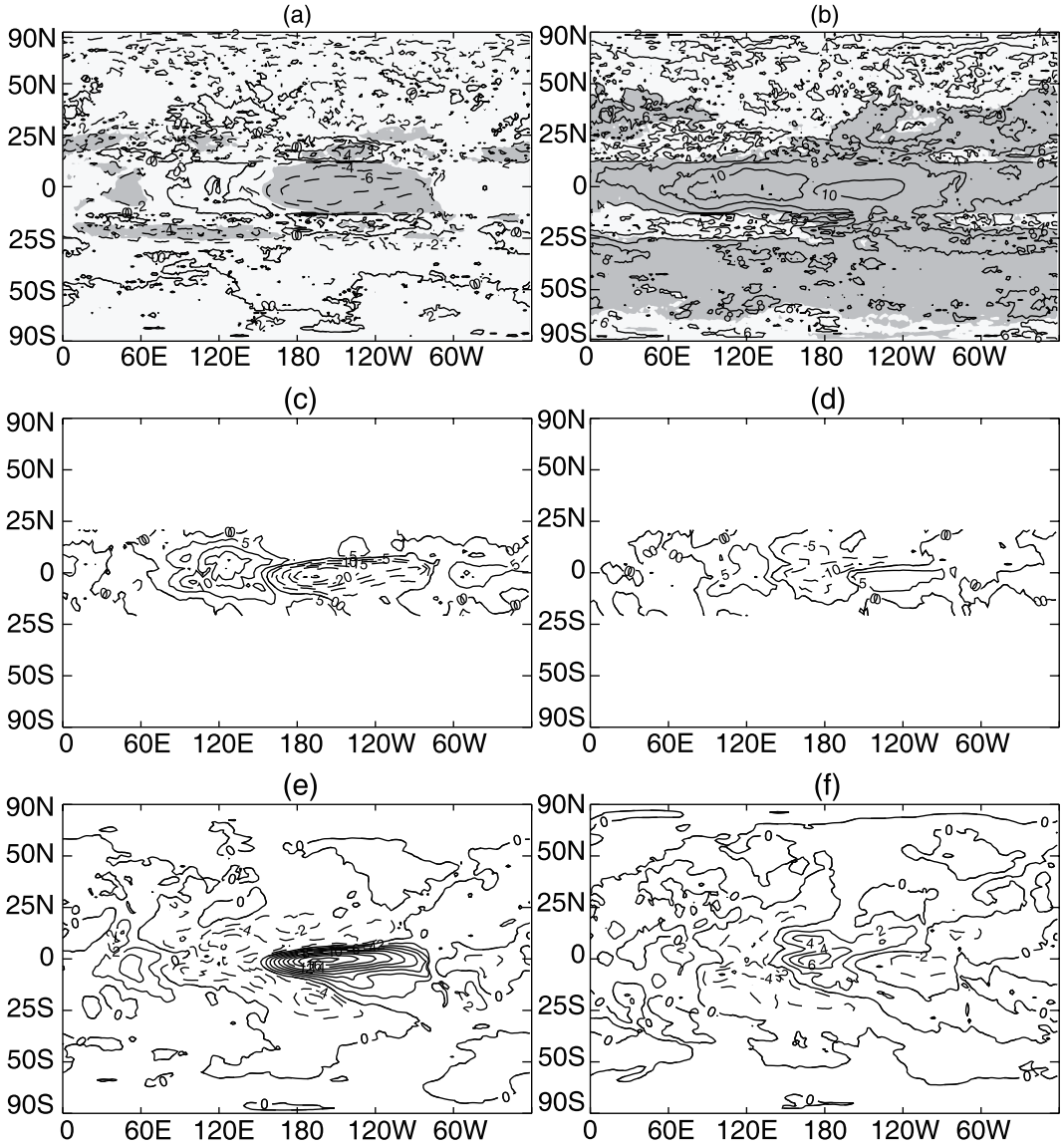

Fig. 9. Latitude–longitude cross sections of tropospheric column ozone anomalies (%) composited from 1980–2010 ERA-Interim data for (a) canonical El Niño events and (b) El Niño Modoki events. Contour intervals are ±2% for ozone anomalies. Solid lines represent positive values; dashed lines represent negative values. Tropospheric column ozone is calculated assuming that the troposphere extends from the tropopause to 1000 hPa. Shaded areas are significant at the 95% confidence level (Student's *t*-test). Latitude–longitude cross sections of tropical OLR anomalies composited from 1980–2010 NOAA data for (c) canonical El Niño events and (d) El Niño Modoki events. Contour intervals are ±3 W m^{-2}. Latitude–longitude cross sections of tropospheric water vapor concentration anomalies averaged from 1000 hPa to 200 hPa composited from 1980–2010 ERA-Interim data for (e) canonical El Niño events and (f) El Niño Modoki events. Contour intervals are ±1000 ppmv. Solid lines represent positive values; dashed lines represent negative values.

pospheric chemistry. Previous studies have pointed out that changes in STE caused by ENSO significantly affect tropospheric ozone (Langford et al., 1998; James et al., 2003; Zeng and Pyle, 2005); however, STE primarily influences ozone in the extratropical troposphere. Changes in the horizontal distribution of tropical convection associated with the two types of El Niño are shown in Figs. 9c and d. Outgoing longwave radiation (OLR) data, represented as an index of convection, from 1980 to 2010 are obtained from the NOAA Climate Data Center (http://www.cdc.noaa.gov/). Due to the water vapor concentration substantially affecting the lifetime of ozone in the troposphere, the anomalies of tropospheric water vapor concentration averaged from 1000 hPa to 200 hPa during the two types of El Niño are also shown in Figs. 9e and f. Convective activity is strengthened in the eastern Pacific and weakened in the western Pacific during canonical El Niño events (Fig. 9c). The water vapor anomalies correspond to the convection anomalies (Figs. 9e and c). These changes in convective activity and water vapor are indeed associated with negative ozone anomalies in the eastern Pacific

and positive ozone anomalies in the western Pacific (Figs. 9e, c and a). However, during El Niño Modoki periods, the water vapor anomalies are associated with convection anomalies, but those anomalies are not in accordance spatially with the ozone anomalies (Figs. 9f, d and b).

Ozone in the troposphere is also affected by UV radiation. Tropospheric ozone production by chemical processes is more efficient when solar radiation is more intense, and vice versa. Stratospheric column ozone changes can therefore affect tropospheric column ozone: decreases in stratospheric column ozone increase the amount of solar UV radiation reaching the troposphere, while increases in stratospheric column ozone decrease the amount of solar UV radiation. We found that tropospheric column ozone is significantly anti-correlated with stratospheric column ozone only in the tropics; the correlation coefficient is -0.67 (Fig. 10). The correlation coefficients between tropospheric column ozone changes and stratospheric column ozone changes in the northern and southern extratropics are -0.13 and 0.11, respectively. This strong anti-correlation implies that the intensity of UV radiation can influence tropospheric ozone changes in the tropics, and represents the possible mechanism of stratospheric ozone affecting tropospheric ozone during El Niño Modoki events. Certainly, the mechanism needs further verification.

5. Summary and conclusions

The effects of the two types of El Niño events (canonical El Niño and El Niño Modoki) on global ozone from 1980 to 2010 have been investigated and compared using composite analyses of ERA-Interim reanalysis data and the N3I and EMI data. Canonical El Niño events lead to a positive ozone anomaly at high latitudes in the Northern Hemisphere and a negative ozone anomaly in the tropical lower stratosphere. The pattern of ozone anomalies associated with El Niño Modoki is totally different from those associated with canonical El Niño. This is because El Niño Modoki can more strongly enhance BD circulation compared to canonical El Niño, which transports more ozone-poor air to the lower stratosphere. Significant anomalies in the local meridional circulation over the longitude band of 60°–120°W in both hemispheres during El Niño Modoki periods generate a greater decrease in stratospheric column ozone over the tropical eastern Pacific than over other tropical areas.

El Niño Modoki events significantly increase the tropospheric column ozone, and the possible mechanism for this is changes in stratospheric column ozone affecting tropospheric column ozone in the tropics. Stratospheric column ozone decreases substantially during El Niño Modoki events in the tropics, increasing the intensity of solar UV radiation in the tropical troposphere. The process enhances the efficiency of chemical ozone production in the troposphere and induces a significant positive anomaly in tropospheric column ozone.

The EOF analysis of time series of stratospheric and tropospheric ozone anomalies over the past three decades reveals several key points. In the stratosphere, the leading EOF mode is associated with El Niño Modoki, which accounts for 27% of the total variance, while the second mode corresponds to the QBO, which accounts for 10% of the total variance. The leading EOF mode in the troposphere is also associated with El Niño Modoki, which accounts for 50% of the total variance. The second mode possibly corresponds to NO_x-related chemistry, which accounts for 22% of the total variance. These results indicate that El Niño Modoki has played a key role in controlling the variations of global ozone in the last three decades.

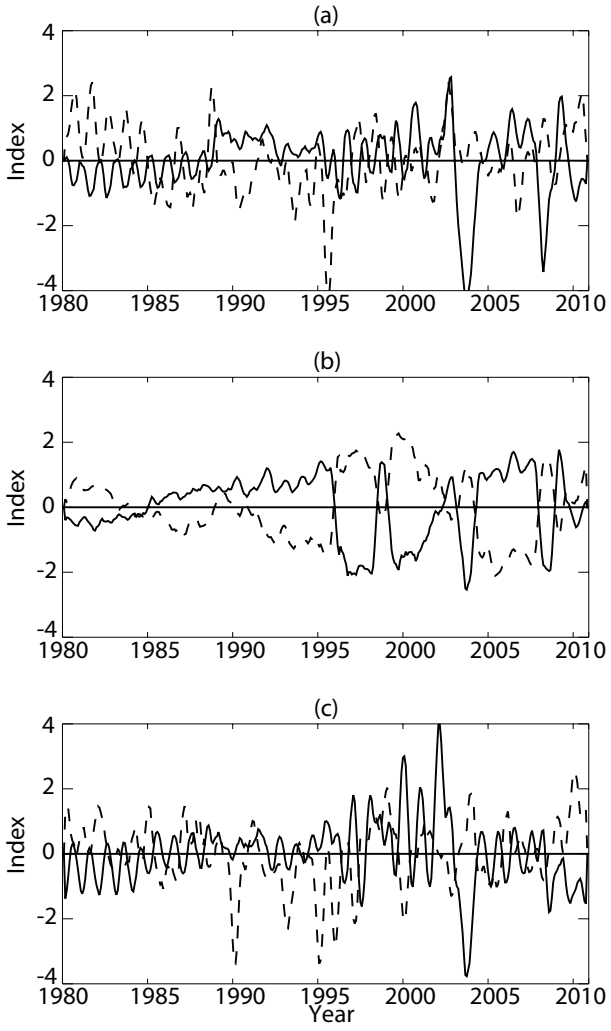

Fig. 10. Normalized variations of stratospheric column ozone (solid line) and tropospheric column ozone (dashed line) anomalies averaged for (a) (25°–90°N, 180°W–180°E), (b) (25°S–25°N, 180°W–180°E), and (c) (25°–90°S, 180°W–180°E). The variations of stratospheric/tropospheric column ozone were obtained by removing the annual cycle and linear trend from the original time series.

Acknowledgements. This work was jointly supported by the 973 Program (Grant No. 2010CB950400) and the National Natural Science Foundation of China (Grant Nos. 41225018 and 41305036).

REFERENCES

Ashok, K., and T. Yamagata, 2009: The El Niño with a difference. *Nature*, **461**, 481–484.

Ashok, K., S. K. Behera, S. A. Rao, H. Weng, and T. Yamagata, 2007: El Niño Modoki and its possible teleconnection. *J. Geophys. Res.*, **112**, C11007, doi: 10.1029/2006JC003798.

Bian, J. C., H. B. Chen, Z. B. Zhang, and Y. L. Zhao, 2005: Unusual discrepancy between TOMS and ground-based measurements of the total ozone in 2002–2003. *Chinese Science Bulletin*, **50**(6), 606–608.

Bian, J. C., G. C. Wang, H. B. Chen, D. L. Qi, D. Lü, and X. Zhou, 2006: Ozone mini-hole occurring over the Tibetan Plateau in December 2003. *Chinese Science Bulletin*, **51**(7), 885–888.

Bian, J., A. Gettelman, H. Chen, and L. Pan, 2007: Validation of satellite ozone profile retrievals using Beijing ozonesonde data. *J. Geophys. Res.*, **112**, D06305, doi: 10.1029/2006JD007502.

Bodeker, G. E., H. Shiona, and H. Eskes, 2005: Indicators of Antarctic ozone depletion. *Atmospheric Chemistry and Physics*, **5**, 2603–2615.

Cagnazzo, C., and Coauthors, 2009: Northern winter stratospheric temperature and ozone responses to ENSO inferred from an ensemble of Chemistry Climate Models. *Atmospheric Chemistry and Physics*, **9**, 8935–8948.

Calvo, N., R. R. Garcia, W. J. Randel, and D. R. Marsh, 2010: Dynamical mechanism for the increase in tropical upwelling in the lowermost tropical stratosphere during warm ENSO events. *J. Atmos. Sci.*, **67**, 2331–2340, doi: 10.1175/2010JAS3433.1.

Camp, C. D., and K. K. Tung, 2007: Stratospheric polar warming by ENSO in winter: A statistical study. *Geophys. Res. Lett.*, **34**, L04809, doi: 10.1029/2006GL028521.

Chen, Y., H. Zhang, and X. Q. Bi, 1998: A numerical experiment on the impact of antartic ozone hole on the global climate. *Journal of China University of Science and Technology*, **6**, 664–668. (in Chinese)

Chen, Y. J., B. Zheng, and H. Zhang, 2002: The features of ozone quasi-biennial oscillation in tropical stratosphere and its numerical simulation. *Adv. Atmos. Sci.*, **19**, 777–793.

Chen, Y. J., C. H. Shi, and B. Zheng, 2005: HCl quasi-biennial oscillation in the stratosphere and a comparison with ozone QBO. *Adv. Atmos. Sci.*, **22**(5), 751–758.

Chen, Y. J., C. H. Shi, R. J. Zhou, and Y. Bi, 2006: Contents and trends of the trace gases in the stratosphere over China. *Chinese Journal of Geophysical*, **49**(5), 1288–1297. (in Chinese)

Chandra, S., J. R. Ziemke, W. Min, and W. G. Read, 1998: Effects of 1997–1998 El Niño on tropospheric ozone and water vapor. *Geophys. Res. Lett.*, **25**, 3867–3870.

Chandra, S., J. R. Ziemke, P. K. Bhartia, and R. V. Martin, 2002: Tropical tropospheric ozone: Implications for dynamics and biomass burning. *J. Geophys. Res.*, **107**, 4188, doi: 10.1029/2001JD000447.

Chandra, S., J. R. Ziemke, M. R. Schoeberl, L. Froidevaux, W. G. Read, P. F. Levelt, and P. K. Bhartia, 2007: Effects of the 2004 El Niño on tropospheric ozone and water vapor. *Geophys. Res. Lett.*, **34**, L06802, doi: 10.1029/2006GL028779.

Chandra, S., J. R. Ziemke, B. N. Duncan, T. L. Diehl, N. J. Livesey, and L. Froidevaux, 2009: Effects of the 2006 El Niño on tropospheric ozone and carbon monoxide: Implications for dynamics and biomass burning. *Atmospheric Chemistry and Physics*, **9**, 4239–4249, doi: 10.5194/acp-9–4239-2009.

Crooks, S. A., and L. J. Gray, 2005: Characterization of the 11-year solar signal using a multiple regression analysis of the ERA-40 dataset. *J. Climate*, **18**, 996–1015.

Doherty, R. M., D. S. Stevenson, C. E. Johnson, W. J. Collins, and M. G. Sanderson, 2006: Tropospheric ozone and El Niño-Southern Oscillation: Influence of atmospheric dynamics, biomass burning emissions, and future climate change. *J. Geophys. Res.*, **111**, D19304, doi: 10.1029/2005JD006849.

Dragani, R., 2011: On the quality of the ERA-Interim ozone reanalyses: Comparisons with satellite data. *Quart. J. Roy. Meteor. Soc.*, **137**, 1312–1326. doi: 10.1002/qj.821.

Edmon, H. J., B. J. Hoskins, and M. E. McIntyre, 1980: Eliassen-Palm cross sections for the troposphere. *J. Atmos. Sci.*, **37**, 2600–2616.

Eyring, V., T. G. Shepherd, and D. W. Waugh, Eds., 2010: SPARC report on the evaluation of chemistry-climate models. SPARC Rep. 5, WCRP-132, WMO/TD-1526, SPARC, World Clim. Res. Programme, World Meteorol. Org., Geneva, 425 pp.

Feng, J., and J. P. Li, 2011: Influence of El Niño Modoki on spring rainfall over south China. *J. Geophys. Res.*, **116**, D13102, doi: 10.1029/2010JD015160.

Fischer, A. M., D. T. Shindell, B. Winter, M. S. Bourqui, G. Faluvegi, E. Rozanov, M. Schraner, and S. Brönnimann, 2008: Stratospheric winter climate response to ENSO in three chemistry-climate models. *Geophys. Res. Lett.*, **35**, L13819, doi: 10.1029/2008GL034289.

Free, M., and D. J. Seidel, 2009: The observed El Niño-Southern Oscillation temperature signal in the stratosphere. *J. Geophys. Res.*, **114**, D23108, doi: 10.1029/2009JD012420.

Fujiwara, M., K. Kita, T. Ogawa, S. Kawakami, T. Sano, N. Komala, S. Saraspriya, and A. Suripto, 2000: Seasonal variation of tropospheric ozone in Indonesia revealed by 5-year ground-based observations. *J. Geophys. Res.*, **105**, 1879–1888.

García-Herrera, R., N. Calvo, R. R. Garcia, and M. A. Giorgetta, 2006: Propagation of ENSO temperature signals into the middle atmosphere: A comparison of two general circulation models and ERA-40 reanalysis data. *J. Geophys. Res.*, **111**, D06101, doi: 10.1029/2005JD006061.

Garfinkel, C. I., and D. L. Hartmann, 2007: Effects of El Niño-Southern oscillation and the quasi-biennial oscillation on polar temperatures in the stratosphere. *J. Geophys. Res.*, **112**, D19112, doi: 10.1029/2007JD008481.

Gettelman, A., W. J., Randel, S., Massie, F., Wu, W. G. Read, and J. M. Tussell III, 2001: El Niño as a natural experiment for studying the tropical tropopause region. *J. Climate*, **14**, 3375–3392.

Hamilton, K., 1993: An examination of observed Southern oscillation effects in the Northern Hemisphere stratosphere. *J. Atmos. Sci.*, **50**, 3468–3473.

Hauglustaine, D. A., G. P. Brasseur, and J. S. Levine, 1999: A sensitivity simulation of tropospheric ozone changes due to the 1997 Indonesian fire emissions. *Geophys. Res. Lett.*, **26**, 3305–3308.

Hood, L. L., B. E. Soukharev, and J. P. McCormack, 2010: Decadal variability of the tropical stratosphere: Secondary influence of the El Niño-Southern Oscillation. *J. Geophys. Res.*, **115**, D11113, doi: 10.1029/2009JD012291.

Hu, Y. Y., and K. K. Tung, 2003: Possible ozone induced long-term change in planetary wave activity in late winter. *J. Climate*, **16**, 3027–3038.

Hu, Y. Y., and Q. Fu, 2009: Stratospheric warming in Southern Hemisphere high latitudes since 1979. *Atmospheric Chem-*

istry and Physics, **9**, 4329–4340.

Hu, Y. Y., and L. F. Pan, 2009: Arctic stratospheric winter warming forced by observed SSTs. *Geophys. Res. Lett.*, **36**, L11707, doi: 10.1029/2009GL037832.

Hurwitz, M. M., P. A. Newman, L. D. Oman, and A. M., Molod, 2011a: Response of the Antarctic stratosphere to two types of El Niño events. *J. Atmos. Sci.*, **68**, 812–822, doi: 10.1175/2011JAS3606.1.

Hurwitz, M. M, I. S. Song, L. D. Oman, P. A. Newman, A. M. Molod, S. M. Frith, and J. E. Nielsen, 2011b: Response of the antarctic stratosphere to warm pool El Niño events in the GEOS CCM. *Atmospheric Chemistry and Physics*, **11**, 9659–9669, doi: 10.5194/acp-11-9659-2011.

James, P., A. Stohl, C. Forster, S. Eckhardt, P. Seibert, and A. Frank, 2003: A 15-year climatology of stratosphere-troposphere exchange with a Lagrangian particle dispersion model: 2. Mean climate and seasonal variability. *J. Geophys. Res.*, **108**, 8522, doi: 10.1029/2002JD002639.

Kley, D., P. J. Crutzen, H. G. J. Smit, H. Vomel, S. J. Oltmans, H. Grassl, and V. Ramanathan, 1996: Observations of nearzero ozone concentrations over the convective Pacific: Effects on air chemistry. *Science*, **274**, 230–233, doi: 10.1126/science.274.5285.230.

Kiladis, G. N., K. H. Straub, G. C. Reid, and K. S. Gage, 2001: Aspects of interannual and intraseasonal variability of the tropopause and lower stratosphere. *Quart. J. Roy. Meteor. Soc.*, **127**, 1961–1983.

Langford, A. O., T. J. O'Leary, C. D. Masters, K. C. Aikin, and M. H. Proffitt, 1998: Modulation of middle and upper tropospheric ozone at northern midlatitudes by the El Niño/Southern Oscillation. *Geophys. Res. Lett.*, **25**, 2667–2670.

Lee, H., and A. K. Smith, 2003: Simulation of the combined effects of solar cycle, quasi-biennial oscillation, and volcanic forcing on stratospheric ozone changes in recent decades. *J. Geophys. Res.*, **108**(D2), 4049, doi: 10.1029/2001JD001503.

Lee, S., D. M. Shelow, A. M. Thompson, and S. K. Miller, 2010: QBO and ENSO variability in temperature and ozone from SHADOZ, 1998–2005. *J. Geophys. Res.*, **115**, D18105, doi: 10.1029/2009JD013320.

Liao, H., and J. H. Seinfeld, 2005: Global impacts of gas-phase chemistry-aerosol interactions on direct radiative forcing by anthropogenic aerosols and ozone. *J. Geophys. Res.*, **110**, D18208, doi: 10.1029/2005JD005907.

Liao, H., J. H. Seinfeld, P. J. Adams, and L. J. Mickley, 2004: Global radiative forcing of coupled tropospheric ozone and aerosols in a unified general circulation model. *J. Geophys. Res.*, **109**, D16207, doi: 10.1029/2003JD004456.

Liao, H., W. T. Chen, and J. H. Seinfeld, 2006: Role of climate change in global predictions of future tropospheric ozone and aerosols. *J. Geophys. Res.*, **111**, D12304, doi: 10.1029/2005JD006852.

Lin, P., Q. Fu, and D. L. Hartmann, 2012: Impact of tropical SST on stratospheric planetary waves in the Southern Hemisphere. *J. Climate*, **25**, doi: 10.1175/JCLI-D-11-00378.1.

Liu, Y., Y. Wang, X. Liu, Z. N. Cai, and K. Chance, 2009a: Tibetan middle tropospheric ozone minimum in June discovered from GOME observations. *Geophys. Res. Lett.*, **36**(5), 1–6.

Liu, Y., C. X. Liu, H. P. Wang, X. X. Tie, S. T. Gao, D. Kinnison, and G. Brasseur, 2009b: Atmospheric tracers during the 2003–2004 stratospheric warming event and impact of ozone intrusions in the troposphere. *Atmospheric Chemistry and Physics*, **9**, 2157–2170.

Liu, Y., C. H. Lu, Y. Wang, and E. Kyrölä, 2011: The quasi-biennial and semi-annual oscillation features of tropical O_3, NO_2, and NO_3 revealed by GOMOS satellite observations for 2002–2008. *Chinese Science Bulletin*, **56**, 1921–1929.

Manzini, E., M. A. Giorgetta, M. Esch, L. Kornblueh, and E. Roeckner, 2006: The influence of sea surface temperatures on the Northern winter stratosphere: Ensemble simulations with the MAECHAM5 model. *J. Climate*, **19**(6) 3863–3881.

Newell, R. E., Y. Zhu, E. V. Browell, W. G. Read, and J. W. Waters, 1996: Walker circulation and tropical upper tropospheric water vapor. *J. Geophys. Res.*, **101**, 1961–1974.

Oman, L. D., J. R. Ziemke, A. R. Douglass, D. W. Waugh, C. Lang, J. M. Rodriguez, and J. E. Nielsen, 2011: The response of tropical tropospheric ozone to ENSO. *Geophys. Res. Lett.*, **38**, L13706, doi: 10.1029/2011GL047865.

Philander, S. G., 1990: *El Niño, La Niña and the Southern Oscillation*. Academic Press, 293 pp.

Quan, X. W., H. F. Diaz, and M. P. Hoerling, 2004: Change in the tropical Hadley cell since 1950. *The Hadley Circulation: Past, Present, and Future*, H. F. Diaz and R. S. Bradley, Eds., Cambridge Univ. Press, 85–120.

Randel, W. J., and F. Wu, 1996: Isolation of the ozone QBO in SAGE II data by singular-Value decomposition. *J. Atmos. Sci.*, **53**(17), 2546–2559.

Randel, W. J., and F. Wu, 2007: A stratospheric ozone profile data set for 1979–2005: Variability, trends, and comparisons with column ozone data. *J. Geophys. Res.*, **112**, D06313, doi: 10.1029/2006JD007339.

Randel, W. J., and A. M. Thompson, 2011: Interannual variability and trends in tropical ozone derived from SAGE II satellite data and SHADOZ ozonesondes. *J. Geophys. Res.*, **116**, D07303, doi: 10.1029/2010JD015195.

Randel, W. J., F. Wu, and D. J. Gaffen, 2000: Interannual variability of the tropical tropopause derived from radiosonde data and NCEP reanalysis. *J. Geophys. Res.*, **105**, 15509–15523.

Randel, W. J., R. R. Garcia, N. Calvo, and D. Marsh, 2009: ENSO influence on zonal mean temperature and ozone in the tropical lower stratosphere. *Geophys. Res. Lett.*, **36**, L15822, doi: 10.1029/2009GL039343.

Rasmusson, E. M., and T. H. Carpenter, 1982: Variations in tropical sea surface temperature and surface wind fields associated with the Southern Oscillation/El Niño. *Mon. Wea. Rev.*, **110**, 354–384, doi: 10.1175/1520-0493(1982)110<0354:VITSST>2.0.CO;2.

Reid, G. C., and K. S. Gage, 1985: Interannual variations in the height of the tropical tropopause. *J. Geophys. Res.*, **90**, 5629–5635.

Renwick, J. A., and M. J. Revell, 1999: Blocking over the South Pacific and Rossby wave propagation. *Mon. Wea. Rev.*, **127**, 2233–2247.

Sassi, F., D. Kinnison, B. A. Boville, R. R. Garcia, and R. Roble, 2004: Effect of El Niño-southern oscillation on the dynamical, thermal, and chemical structure of the middle atmosphere. *J. Geophys. Res.*, **109**, D17108, doi: 10.1029/2003JD004434.

Shi, C. H., B. Zheng, and S. S. Zhong, 2007: The relationships between the zonal temperature variation and ozone distribution in the Northern Hemisphere winter stratosphere. *Proc. of SPIE*, 6681, doi: 10.1117/12.735313.

Shi, C. H., Y. J. Chen, B. Zheng, and Y. Liu, 2010: A comparison of the contributions of dynamical transportation and

photochemical process to ozone's seasonal variation in the stratosphere. *Chinese J. Atmos. Sci.*, **34**(2), 399–406, doi: 10.3878/j.issn.1006-9895.2010.02.13. (in Chinese)

Simmons, A., S. Uppala, D. Dee, and S. Kobayashi, 2007a: ERAInterim: New ECMWF reanalysis products from 1989 onwards. *ECMWF Newsletter*, **110**, 25–25.

Simmons, A., S. Uppala, and D. Dee, 2007b: Update on ERAInterim. *ECMWF Newsletter*, **111**, 5.

Sudo, K., and M. Takahashi, 2001: Simulation of tropospheric ozone changes during 1997–1998 El Niño: Meteorological impact on tropospheric photochemistry. *Geophys. Res. Lett.*, **28**, 4091–4094, doi: 10.1029/2001GL013335.

Taguchi, M., and Hartmann, D. L., 2006: Increased occurrence of stratospheric sudden warmings during El Niño as simulated by WACCM. *J. Climate*, **19**, 324–332.

Thompson, A. M., and R. D. Hudson, 1999: Tropical tropospheric ozone (TTO) maps from Nimbus 7 and Earth Probe TOMS by the modified-residual method: Evaluation with sondes, ENSO signals, and trends from Atlantic regional time series. *J. Geophys. Res.*, **104**, 26 961–26 975.

Thompson, A. M., J. C. Witte, R. D. Hudson, H. Guo, J. R. Herman, and M. Fujiwara, 2001: Tropical tropospheric ozone and biomass burning. *Science*, **291**, 2128–2132, doi: 10.1126/science.291.5511.2128.

Trenberth, K. E., 1997: The definition of El Niño. *Bull. Amer. Meteor. Soc.*, **78**, 2771–2777, doi: 10.1175/1520–0477(1997)078<2771:TDOENO>2.0.CO;2.

Trenberth, K. E., and L. Smith, 2006: The vertical structure of temperature in the tropics: Different flavors of El Niño. *J. Climate*, **19**, 4956–4970.

Trenberth, K. E., and L. Smith, 2009: Variations in the three-dimensional structure of the atmospheric circulation with different flavors of El Niño. *J. Climate*, **22**, 2978–2991.

Uppala, S., D. Dee, S. Kobayashi, P. Berrisford, and A. Simmons, 2008: Towards a climate data assimilation system: Status update of ERA-Interim. *ECMWF Newsletter*, **115**, 12–18.

van Loon, H., and K. Labitzke, 1987: The Southern Oscillation. Part V: The anomalies in the lower stratosphere of the Northern Hemisphere in winter and a comparison with the quasi-biennial oscillation. *Mon. Wea. Rev.*, **115**, 357–369.

Weng, H. Y., S. K. Behera, and T. Yamagata, 2009: Anomalous winter climate conditions in the Pacific rim during recent El Niño Modoki and El Niño events. *Climate Dyn.*, **32**, 663–674, doi: 10.1007/s00382-008-0394-6.

Xie, F., W. S. Tian, J. Austin, J. Li, H. Y. Tian, J. C. Shu, and C. Chen, 2011: The effect of ENSO activity on lower stratospheric water vapor. *Atmospheric Chemistry and Physics*, **11**, 4141–4166, doi: 10.5194/acpd-11-4141-2011.

Xie, F., J. Li, W. Tian J. Feng, and Y. Hou, 2012: The signals of El Niño modoki in the tropical tropopause layer and stratosphere. *Atmospheric Chemistry and Physics*, **12**, 5259–5273, doi: 10.5194/acp-12-5259-2012.

Yeh, S. J. Kug, B. Dewitte, M. Kwon, B. Kirtman, and F. Jin, 2009: El Niño in a changing climate. *Nature*, **461**, 511–514.

Yulaeva, E., J. R. Holton, and J. M. Wallace, 1994: On the cause of the annual cycle in tropical lower-stratospheric temperature. *J. Atmos. Sci.*, **51**, 169–174.

Zeng, G., and J. A. Pyle, 2005: Influence of El Niño Southern oscillation on stratosphere/troposphere exchange and the global tropospheric ozone budget. *Geophys. Res. Lett.*, **32**, L01814, doi: 10.1029/2004GL021353.

Zhang, W. J., J. P. Li, and F. F. Jin, 2009: Spatial and temporal features of ENSO meridional scales. *Geophys. Res. Lett.*, **36**, L15605, doi: 10.1029/2009GL038672.

Zhang, W. J., J. P. Li, and X. Zhao, 2010: Sea surface temperature cooling mode in the Pacific cold tongue. *J. Geophys. Res.*, **115**, C12042, doi: 10.1029/2010JC006501.

Zheng, B., Y. J. Chen, and J. Jian, 2003a: Quasi-biennial oscillation in NOx and its relation to quasi-biennial oscillation in O_3, Part I: Data analysis. *Chinese J. Atmos. Sci.*, **27**(3), 280–292. (in Chinese)

Zheng, B., Y. J. Chen, and H. Zhang, 2003b: Quasi-biennial oscillation in NO_x and its relation to quasi-biennial oscillation in O_3, Part II: Numerical experiment. *Chinese J. Atmos. Sci.*, **27**(4), 387–398. (in Chinese)

Ziemke, J. R., and S. Chandra, 2003: La Nina and El Niño-nduced variabilities of ozone in the tropical lower atmosphere during 1970–2001. *Geophys. Res. Lett.*, **30**, 1142, doi: 10.1029/2002GL016387.

Ziemke, J. R., S. Chandra, L. D. Oman, and P. K. Bhartia, 2010: A new ENSO index derived from satellite measurements of column ozone. *Atmospheric Chemistry and Physics*, **10**, 3711–3721, doi: 10.5194/acp-10-3711-2010.

Zubiaurre, I., and N. Calvo, 2012: The El Niño-Southern Oscillation (ENSO) Modoki signal in the stratosphere. *J. Geophys. Res.*, **117**, D04104, doi: 10.1029/2011JD016690.